



HAL
open science

Meg3 Non-coding RNA Expression Controls Imprinting by Preventing Transcriptional Upregulation in cis

Ildem Sanli, Sébastien Lalevée, Marco Cammisa, Aurélien Perrin, Florence Rage, David Llères, Andrea Riccio, Edouard Bertrand, Robert Feil

► To cite this version:

Ildem Sanli, Sébastien Lalevée, Marco Cammisa, Aurélien Perrin, Florence Rage, et al.. Meg3 Non-coding RNA Expression Controls Imprinting by Preventing Transcriptional Upregulation in cis. *Cell Reports*, 2018, 23 (2), pp.337-348. 10.1016/j.celrep.2018.03.044 . hal-02343524

HAL Id: hal-02343524

<https://hal.science/hal-02343524>

Submitted on 31 May 2021

HAL is a multi-disciplinary open access archive for the deposit and dissemination of scientific research documents, whether they are published or not. The documents may come from teaching and research institutions in France or abroad, or from public or private research centers.

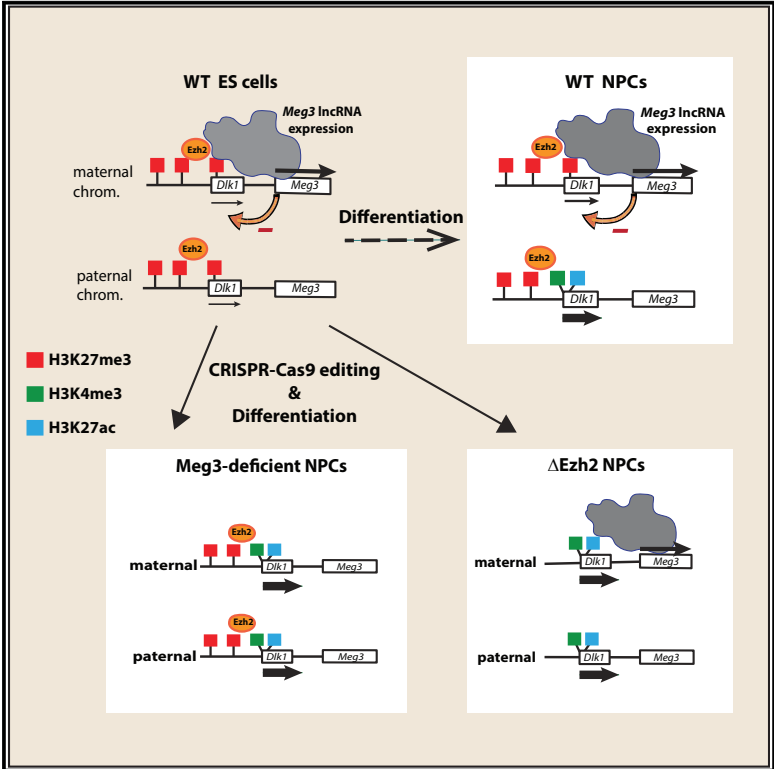
L'archive ouverte pluridisciplinaire **HAL**, est destinée au dépôt et à la diffusion de documents scientifiques de niveau recherche, publiés ou non, émanant des établissements d'enseignement et de recherche français ou étrangers, des laboratoires publics ou privés.



Distributed under a Creative Commons Attribution - NonCommercial - NoDerivatives 4.0 International License

Meg3 Non-coding RNA Expression Controls Imprinting by Preventing Transcriptional Upregulation *in cis*

Graphical Abstract



Authors

Ildem Sanli, Sébastien Lalevée, Marco Cammisa, ..., Andrea Riccio, Edouard Bertrand, Robert Feil

Correspondence

robert.feil@igmm.cnrs.fr

In Brief

Sanli et al. show that the *Dik1* gene becomes imprinted through upregulation of the paternal allele. The maternal allele remains poised during development, and this is controlled by *Meg3* IncRNA expression. Additionally, Ezh2 contributes to the repression of the maternal *Dik1*, although its recruitment is biallelic and independent of *Meg3*.

Highlights

- *Dik1* imprinting arises through developmental activation of the paternal allele
- *Meg3* IncRNA expression prevents *Dik1* activation on the maternal chromosome
- *Meg3* IncRNA is partially retained *in cis* and overlaps the maternal *Dik1* gene
- Both *Meg3* and KMT Ezh2 prevent *Dik1* activation

Data and Software Availability

GSE99903



Meg3 Non-coding RNA Expression Controls Imprinting by Preventing Transcriptional Upregulation *in cis*

Ildem Sanli,^{1,4,5} Sébastien Lalevée,^{1,4} Marco Cammisa,^{2,3} Aurélien Perrin,¹ Florence Rage,¹ David Lières,¹ Andrea Riccio,^{2,3} Edouard Bertrand,¹ and Robert Feil^{1,6,*}

¹Montpellier Institute of Molecular Genetics (IGMM), CNRS and the University of Montpellier, 34293 Montpellier, France

²Institute of Genetics and Biophysics “A. Buzzati-Traverso” (IGB), CNR, 80131 Naples, Italy

³Department of Environmental, Biological and Pharmaceutical Sciences and Technologies (DiSTABiF), Università della Campania “Luigi Vanvitelli,” 81100 Caserta, Italy

⁴These authors contributed equally

⁵Present address: Department of Developmental and Stem Cell Biology, Institut Pasteur, 75015 Paris, France

⁶Lead Contact

*Correspondence: robert.feil@igmm.cnrs.fr
<https://doi.org/10.1016/j.celrep.2018.03.044>

SUMMARY

Although many long non-coding RNAs (lncRNAs) are imprinted, their roles often remain unknown. The *Dlk1-Dio3* domain expresses the lncRNA *Meg3* and multiple microRNAs and small nucleolar RNAs (snoRNAs) on the maternal chromosome and constitutes an epigenetic model for development. The domain's *Dlk1* (Delta-like-1) gene encodes a ligand that inhibits Notch1 signaling and regulates diverse developmental processes. Using a hybrid embryonic stem cell (ESC) system, we find that *Dlk1* becomes imprinted during neural differentiation and that this involves transcriptional upregulation on the paternal chromosome. The maternal *Dlk1* gene remains poised. Its protection against activation is controlled *in cis* by *Meg3* expression and also requires the H3-Lys-27 methyltransferase *Ezh2*. Maternal *Meg3* expression additionally protects against *de novo* DNA methylation at its promoter. We find that *Meg3* lncRNA is partially retained *in cis* and overlaps the maternal *Dlk1* in embryonic cells. Combined, our data evoke an imprinting model in which allelic lncRNA expression prevents gene activation *in cis*.

INTRODUCTION

The *Dlk1-Dio3* imprinted domain is controlled by an intergenic “imprinting control region” (ICR) and plays diverse roles in development and metabolism. This large domain (Figure 1A) comprises three protein-coding genes, *Dlk1* (also called *Pref1*), *Rtl1*, and *Dio3*, whose imprinted expression is tissue-specific and from the paternal chromosome predominantly. The maternal chromosome expresses multiple non-coding RNAs (ncRNAs), including the long ncRNA (lncRNA) *Meg3* (maternally expressed gene 3, also called *Gtl2*), the *Rtl1*-antisense *Rtl1as*, the C/D-box snoRNA cluster *Rian*, and the microRNA cluster *Mirg* (da Rocha et al., 2008).

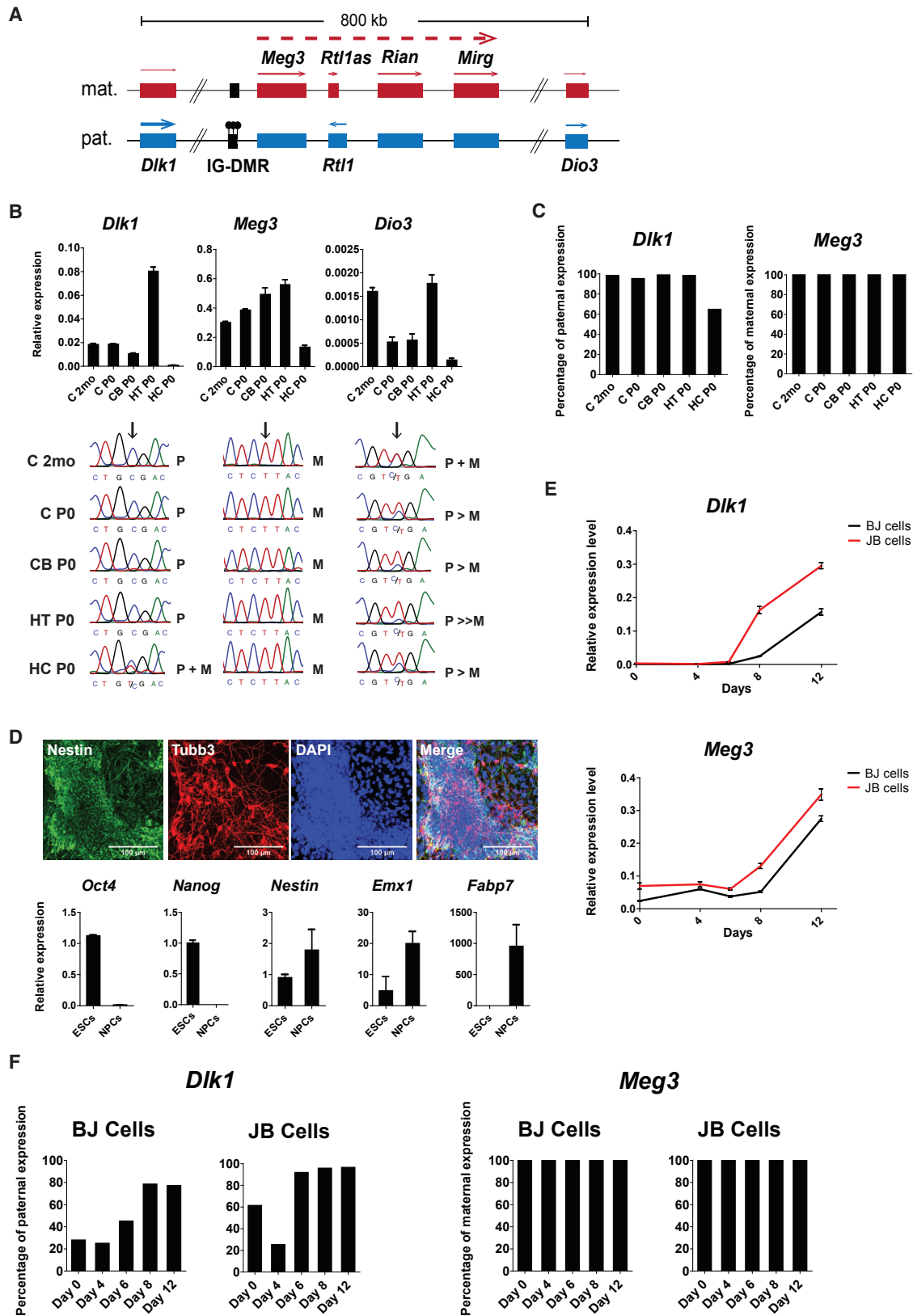
The domain's ICR—called the IG-DMR—is essential for the allelic expression of the ncRNAs and protein-coding genes (Lin et al., 2003). On the maternal chromosome, the ICR is hypomethylated, displays enhancer features, and activates *Meg3* during preimplantation development (Kota et al., 2014; Luo et al., 2016; Wang et al., 2017b). The maternal *Rtl1* allele is repressed by the anti-sense transcript *Rtl1as* and this is important for placental development (Ito et al., 2015). How the preferential paternal expression of *Dlk1* and *Dio3* is controlled is less clear. *Dlk1* and *Dio3* are not known to be controlled by antisense transcription and are positioned further away from the IG-DMR. Despite several studies (Takahashi et al., 2009; Zhou et al., 2010), the imprinting mechanism remains unclear.

Dlk1 is imprinted in many tissues and encodes an antagonistic Notch ligand that plays roles in placental development, nutrient metabolism, and adipocytosis (Charalambous et al., 2014; Moon et al., 2002). *Dio3* imprinted expression is less pronounced than that of *Dlk1*, including in brain tissues (Yevtodiyyenko et al., 2002).

It has been postulated that one of the locus' ncRNAs could repress *Dlk1* on the maternal chromosome (da Rocha et al., 2008). The *Mirg* miRNAs are cytoplasmic, control neonatal metabolic adaptation and mitochondrial metabolism, and do not influence *Dlk1* imprinted expression (Kameswaran et al., 2014; Labialle et al., 2014). *Rian* small nucleolar RNAs (snoRNAs) are also unlikely candidates given their post-transcriptional role in 2'-O-methylation of RNA (Falaleeva et al., 2017). *Meg3* lncRNA is a potential candidate (Kota et al., 2014). Similarly, as many other nascent and lncRNAs (Davidovich et al., 2013; Kaneko et al., 2013; Wang et al., 2017a; Zhao et al., 2010), it interacts *in vitro* with the lysine methyltransferase (KMT) *Ezh2* and other components of the polycomb repressive complex-2 (PRC2) (Cifuentes-Rojas et al., 2014; Kaneko et al., 2014).

Hybrid embryonic stem cells (ESCs) derived in 2i-medium recapitulate imprinted gene expression during neural differentiation (Bouschet et al., 2017). We applied this experimental system to explore the *Dlk1-Dio3* locus and found that *Dlk1* imprinted expression arises through transcriptional upregulation on the paternal chromosome. This developmental activation is prevented on the maternal chromosome, and *Meg3* lncRNA expression and *Ezh2* play essential roles in this process.





(legend on next page)

RESULTS

Dlk1 Imprinted Expression Arises through Paternal Allele Activation

To explore imprinted gene expression at the *Dlk1-Dio3* domain (Figure 1A), we generated mice that were hybrid between C57BL/6J and *M. m. molossinus* inbred strain JF1. Total RNAs from neonatal (P0) brain tissues were analyzed (Figure 1B). *Dlk1* expression was high in hypothalamus (HT), cortex (C), and cerebellum (CB). Much lower expression was apparent in hippocampus (HC). *Dlk1* expression was paternal in the neonatal brain tissues, but for the lowly expressing hippocampus, where *Dlk1* expression was biallelic (Figures 1C and S1A).

In agreement with earlier studies (Yevtodiyenko et al., 2002), *Dio3* expression was low and largely biallelic in neonatal cortex, cerebellum, and hippocampus, whereas paternally biased expression was observed in neonatal hypothalamus (Figure 1B). Expression of *Meg3*, *Rian*, and *Mirg* was high and maternal allele-specific in all brain tissues analyzed (Figures 1B, 1C, and S1B).

To explore gene expression during differentiation, we derived ESC lines in serum-free 2i-medium that were hybrid between C57BL/6J (B) and JF1 (J). Two of the obtained lines, BJ1-WT3 and JB1-WT6 (hereafter called BJ and JB, respectively), were chosen for further studies, performed on early passages (passages 3–12). Both ESC lines had an unaltered chromosome number (Figure S2A) and could be readily differentiated into neural progenitor cells (NPCs) with perinatal frontal cortex identity. For this, an established procedure was used, with addition of the sonic hedgehog inhibitor cyclopamine (Gaspard et al., 2009). Following 12 days of cortical differentiation, most cells displayed neural morphology with axonal outgrowth and expression of the neural markers *Nestin*, *Tubb3*, *Emx1*, and *Fabp7* (Figure 1D).

Dlk1 expression was very low in undifferentiated ESCs and detected on both parental alleles. Expression levels increased strongly from day 6 of corticogenesis onward. At day 12, the attained levels were comparable to those in neonatal cortex (Figure 1E). In both ESC lines, the kinetics of upregulation correlated with acquisition of paternal allele-specific expression (Figures 1F and S1C). *Dlk1* activation seemed stronger in the JB than in the BJ neural cells, but another JB ESC control line (JB-WT2; Figure S1D) showed comparable *Dlk1* activation as in the BJ cells.

Upon neural differentiation into NPCs, there was a mild increase in *Dio3* expression, which remained biallelic (Figure S1E),

and this agreed with the biallelic expression observed in cortex (Figure 1B). Upon neural differentiation, *Meg3* expression increased moderately and remained strictly maternal (Figures 1E, 1F, and S1C).

To assay whether allelic *Dlk1* activation occurs in other kinds of neural cells as well, ESCs were differentiated with all-trans retinoic acid (RA). This generates neurons and neural progenitors with hindbrain and spinal cord identity (Kim et al., 2009). Again, *Dlk1* imprinting acquisition coincided with the kinetics of the gene's upregulation (Figures S1F and S1G). Combined, these studies indicate that the paternal *Dlk1* allele is strongly upregulated during neural differentiation, whereas expression on the maternal chromosome remains low.

Meg3 Prevents *Dlk1* Upregulation on the Maternal Chromosome

CRISPR-Cas9 technology was used to generate BJ-derived ESC lines with deletions in *Meg3*: a biallelic 198-bp deletion within the *Meg3* promoter (Δ promoter^{-/-}), a 2,195/2,217-bp deletion of the 3' part of intron-1 on the maternal, the paternal, or on both parental chromosomes (Δ intron1^{-/+}, Δ intron1^{+/-}, and Δ intron1^{-/-}, respectively) and a biallelic 29-kb deletion that removed the intron-1 to intron-9 region (Δ intron1-9^{-/-}) (Figure 2A).

The small promoter deletion abolished *Meg3* expression and gave loss of *Rian* and *Mirg* expression (Figure 2B). Absence of the maternal ncRNAs resulted from maternal intron-1 deletion as well. Paternal intron-1 deletion had no effect. Loss of *Meg3*, *Rian*, and *Mirg* expression occurred also in Δ intron1-9^{-/-} ESCs (Figure 2B).

The *Meg3*-targeted ESCs were maintained under serum-free conditions and studied at early passages (4–13), had a normal karyotype (Figure S2A), and could be readily differentiated into NPCs, similarly as the BJ WT ESCs (Figures S2B and S2C).

Meg3-targeted ESCs had unaltered DNA methylation levels at the IG-DMR. However, in the maternal deletion lines, which all showed loss of *Meg3* expression (Figure 2B), there was increased DNA methylation at the *Meg3* promoter (Figure S2D). This suggests that *Meg3* expression contributes to keeping its promoter unmethylated.

The loss of *Meg3* expression did not affect *Dlk1* upregulation during differentiation (Figure S2E). However, *Dlk1* activation was biallelic in the KO NPCs. This "loss of imprinting" (LOI) was apparent in all maternal deletion lines, but not in the Δ intron1^{+/-} line or in non-targeted control cells (Figures 2C and 2D).

Figure 1. *Dlk1* Imprinting Arises through Allelic Upregulation during Differentiation

(A) Schematic presentation of the murine *Dlk1-Dio3* locus. Genes are shown as rectangles with their allelic expression (arrows) state in neonatal cortex. The *Meg3* polycistron is indicated as an interrupted line. The IG-DMR imprinting control region (black box) is methylated (filled lollipops) on the paternal chromosome.

(B) *Dlk1*, *Meg3*, and *Dio3* expression levels in postnatal day 0 (P0) and 2 months (2mo) brain tissues. Levels of expression relative to three housekeeping genes are indicated. Error bars indicate the SEM of qPCR triplicates. Bottom: allele-specificity of expression assayed by Sanger sequencing of RT-PCR products. Arrows indicate SNPs that distinguish maternal (M) and paternal (P) alleles. C, cortex; CB, cerebellum; HT, hypothalamus; HC, hippocampus.

(C) *Dlk1* and *Meg3* expression assayed by quantitative allele-specific PCR.

(D) Immunofluorescence (IF) staining of Tubulin- β 3 and Nestin in NPCs at d12 of cyclopamine-mediated differentiation. Scale bars, 100 μ m. Bottom: relative expression of *Oct4*, *Nanog*, and neural markers in BJ ESC and ESC-derived NPCs (d12); data from three different differentiations, normalized to the levels in ESCs. Error bars represent the SD of three biological replicates.

(E) Relative expression of *Dlk1* and *Meg3* during cyclopamine-mediated differentiation. Error bars indicate the SEM of qPCR triplicates.

(F) Quantitative assessment of allelic *Dlk1* and *Meg3* expression. The allele-specific data (C, E, and F) represent one differentiation experiment.

See also Figure S1.

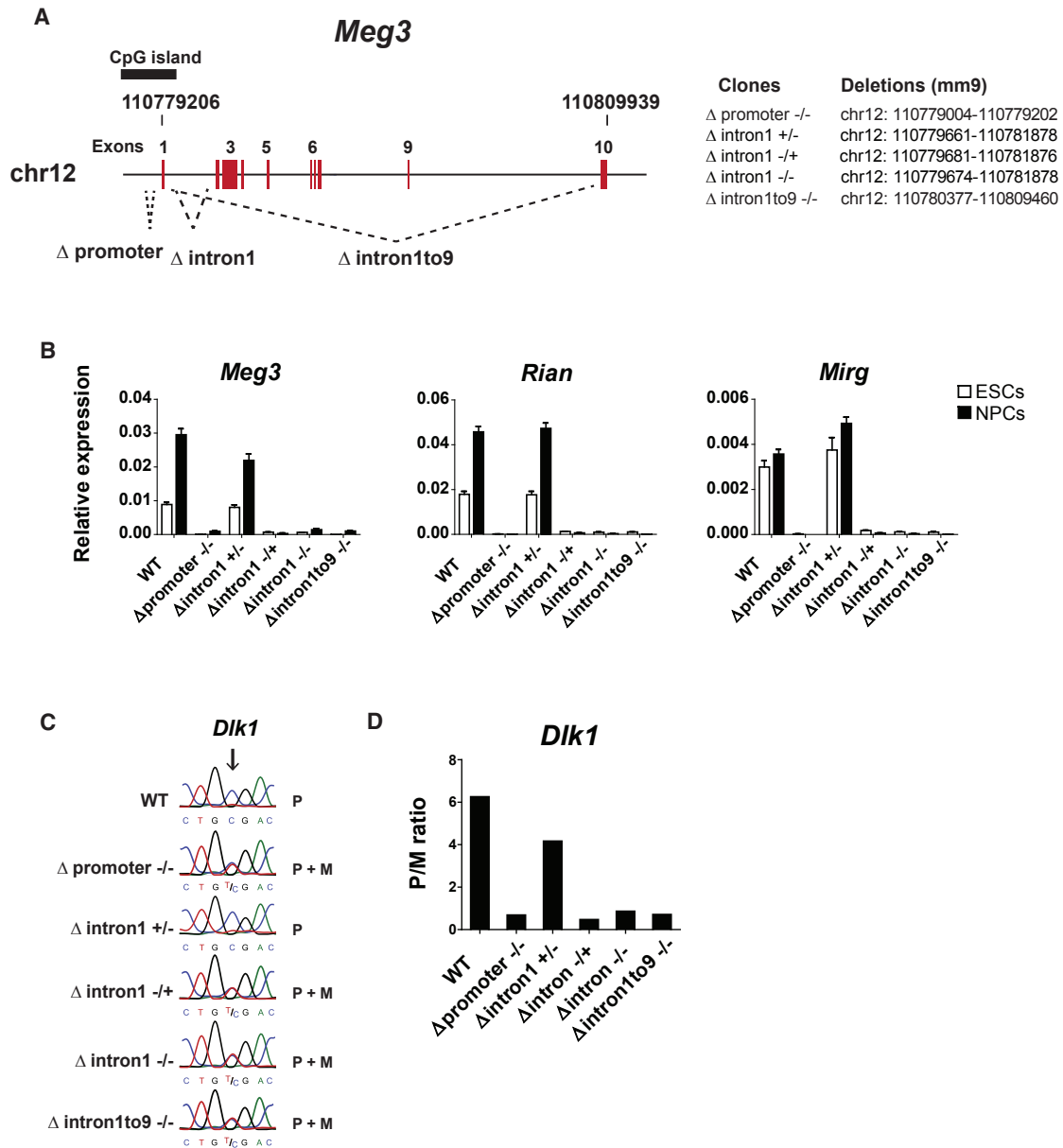


Figure 2. Targeted Deletions within *Meg3* Induce Loss of *Dik1* Imprinting

(A) Map depicting three independent deletions generated by CRISPR-Cas9. Right: the deleted sequence positions (in mm9).

(B) *Meg3*, *Rian*, and *Mirg* expression is abolished as a result of maternal and biallelic deletions within *Meg3*. Expression levels in ESCs and BJ-derived NPCs (day 12) shown in white and black, respectively. Error bars indicate the SEM of qPCR triplicates.

(C) Sanger sequencing-based assessment of *Dik1* expression in the NPCs; the arrow indicates the SNP used to distinguish the maternal (M) and paternal (P) alleles.

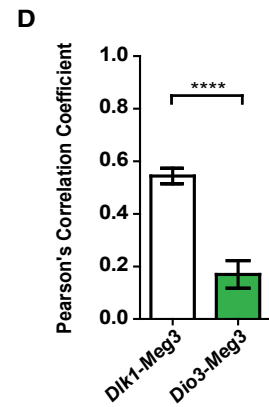
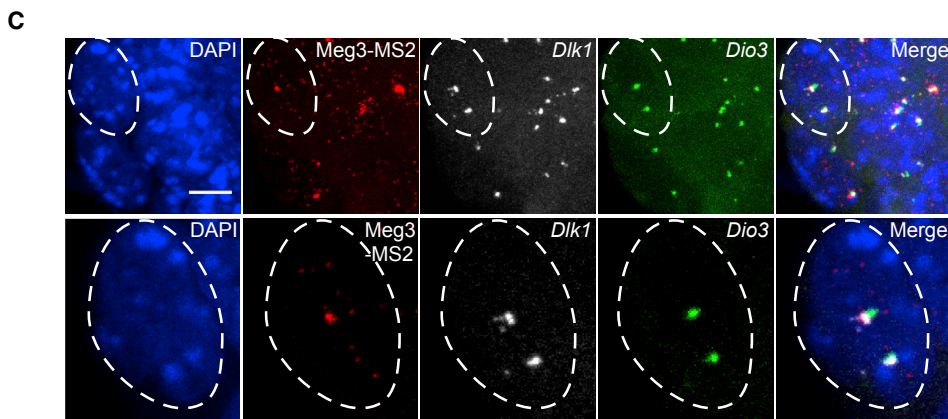
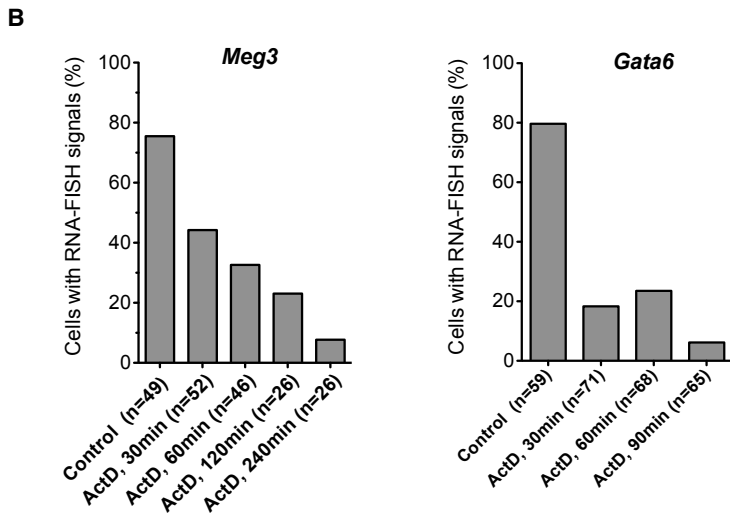
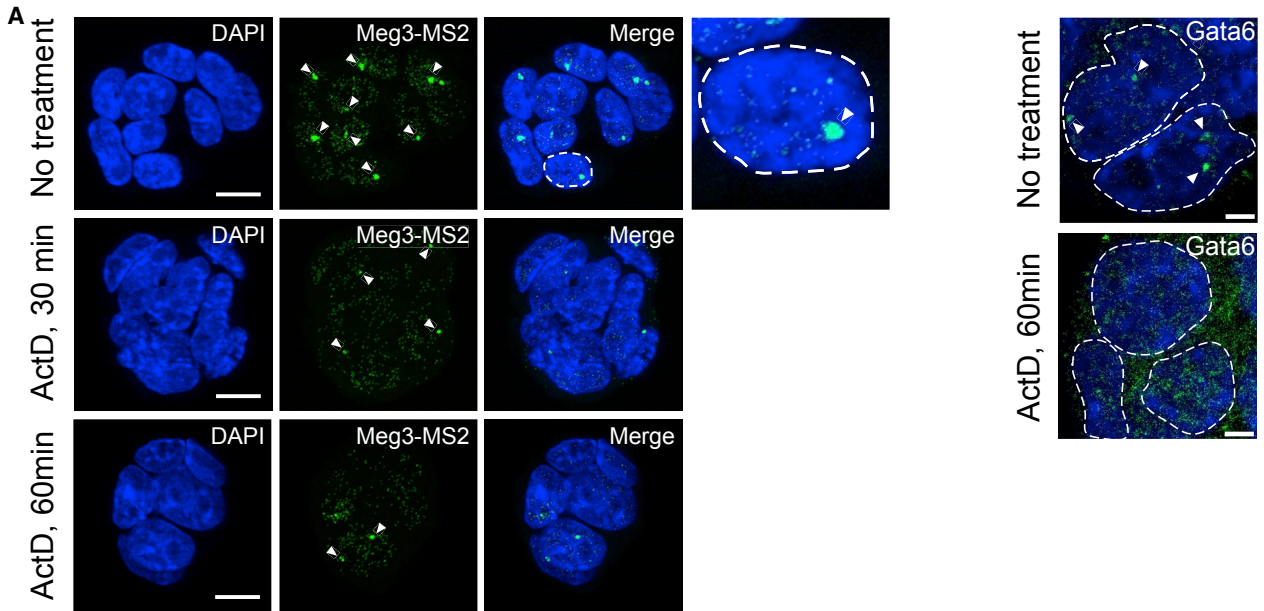
(D) Quantitative assessment of the paternal/maternal ratio of *Dik1* expression in BJ and the *Meg3*-targeted NPCs of one representative differentiation series.

See also Figure S2.

RNA sequencing (RNA-seq) was performed on the wild-type (WT) and Δ promoter $^{-/-}$ and Δ intron1 $^{-/-}$ NPCs (see Supplemental Experimental Procedures). This showed that the allelic expression of *Grb10* and *Kcnq1ot1* (KvDMR1 promoter) and other imprinted genes was unaltered in the *Meg3*-targeted NPCs. RNA-seq also confirmed that the maternal ncRNA genes (*Meg3*, *Rian*, *Mirg*, *AF357359*, and *6430411K18Rik*) of the *Dik1*-

Dio3 domain were no longer expressed in the *Meg3*-targeted NPCs (Figure S2F; Table S5).

Analysis of RNA-seq reads confirmed that *Dik1* expression was paternal in the control and biallelic in the Δ promoter $^{-/-}$ and Δ intron1 $^{-/-}$ NPCs (Figure S2G). All reads at *Dik1* were in the sense orientation, both in WT and Δ promoter $^{-/-}$ and Δ intron1 $^{-/-}$ NPCs. RNA-seq on the Δ promoter $^{-/-}$ and



(legend on next page)

Δ intron1^{-/-} NPCs did not reveal consistent expression changes elsewhere in the genome.

A Fraction of Meg3 RNA Is Retained and Overlaps the Maternal *Dlk1* Gene (*in cis*)

RNA fluorescence *in situ* hybridization (FISH) with a cDNA probe covering exons 1–10 (Figure S3A) showed that Meg3 RNA presents in the majority of ESCs as a unique large focus of 1–2 μ m in diameter (Figures S3B and S3C), on the maternal *Dlk1-Dio3* locus (Kota et al., 2014). To better visualize its nuclear localization, we applied single-molecule inexpensive-FISH (smiFISH) (Tsanov et al., 2016) with fluorophore-tagged, gene-specific, probes covering 24 regions across Meg3. In ESCs, besides a single bright RNA accumulation indicating active transcription site, small spots were apparent elsewhere in the nucleoplasm, likely corresponding to individual Meg3 RNA molecules (Figure S3C). In NPCs, additional foci containing a large number of individual Meg3 RNA signals were apparent in some nuclei, suggestive of dispersion to other nucleoplasmic sites (Figure S3C).

Our own and published RNA-seq data (ESC, NPCs) indicate that *Meg3* expresses different introns at comparable levels as exons, particularly introns 5 and 9 (Figure S3A). Using a probe against intron-9 for RNA FISH, strong single foci were detected that overlapped the ones detected with the cDNA probe (Figures S3A and S3B). Similar data were obtained for introns 5 and 8 (data not shown). This indicates that the main Meg3 RNA foci comprise intronic sequences.

To determine whether Meg3 RNA foci also comprised the small last exon, we inserted 64 (degenerate) tandemly arranged copies of MS2 repeats into exon-10 in BJ ESC cells. Two clones with maternal insertion were obtained. These showed unaltered *Meg3* expression and unaltered DNA methylation at the *Meg3* promoter and the IG-DMR (Figures S3D–S3F). FISH with oligonucleotides designed against the degenerate MS2 copies showed that in each cell, exon-10 RNA was apparent as a large focus that overlapped the cDNA probe signal. Similarly as for smiFISH, also individual small spots were apparent throughout the nucleoplasm, which likely correspond to processed single RNA molecules (Figure S3F). Concordantly, following differentiation into NPCs, imprinted *Dlk1* expression was acquired (Figure S3G).

To further explore the apparent partial retention of Meg3 RNA at the transcription site, we treated the Meg3-MS2 expressing ESCs with the RNA-PolIII inhibitor actinomycin-D (ActD) (Figure 3A) at a concentration (5 μ g/mL) that inhibits transcription within minutes (Bensaude, 2011). In untreated ESCs (control), 75% of the cells showed a large Meg3 RNA focus. After 30 min of ActD treatment, 45% of the cells maintained a bright RNA

focus, and after 60 min of treatment, 37% still did. A control housekeeping gene, *Gata6*, showed a faster disappearance of nascent RNA foci, with only 20% remaining visible after 30 min of treatment (Figures 3A and 3B). The persistence of Meg3 RNA foci upon ActD treatment suggests a partial retention at the transcription site and corroborates our earlier study on the CDK9 inhibitor DRB, which prevents RNA polymerase elongation (Kota et al., 2014).

Next, DNA FISH was performed with a 35-kb fosmid probe comprising *Dlk1* in combination with Meg3 RNA smiFISH (Figure S3C). The spatial relationship of the detected signals was quantified and we calculated the pixel-intensity-based co-localization coefficients using Pearson's correlations. This revealed that the two signals (Meg3 RNA and *Dlk1*) are highly correlated in ESCs (Pearson's coefficient = 0.6). In agreement with the dispersed nature of Meg3 RNA in post-mitotic neural cells, there was less overlap between Meg3 RNA and *Dlk1* in the NPCs (Pearson's coefficient = 0.26) (Figure S3C). The MS2-based RNA-FISH approach showed a similar overlap between Meg3 RNA and *Dlk1* in ESCs (Pearson's coefficient = 0.54). A spatial separation was apparent, however, between the *Dio3* signal and Meg3 RNA in the ESCs (Figures 3C and 3D, Pearson's coefficient = 0.17).

Meg3 Expression Prevents Chromatin Activation on the Maternal *Dlk1* Promoter

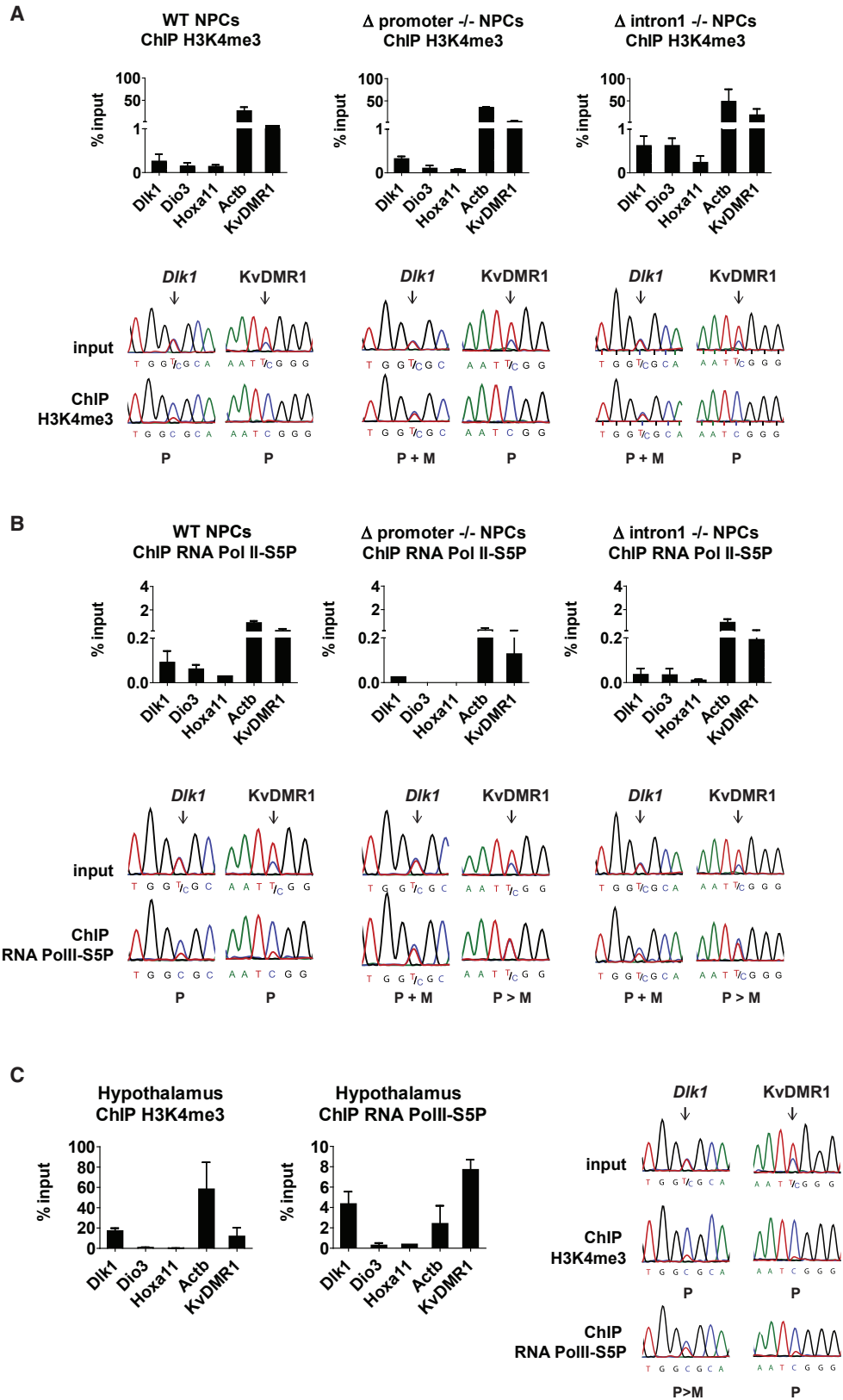
We performed chromatin immunoprecipitation (ChIP) on WT NPCs with an antiserum against H3-lysine-4 tri-methylation (H3K4me3), a marker of active chromatin. At a control imprinted promoter—the KvDMR1 at the *Kcnq1* domain—as expected (Kota et al., 2014), H3K4me3 was enriched on the active paternal allele. At the *Dlk1* promoter, H3K4me3 was precipitated from the paternal allele predominantly in the WT NPCs. In Δ promoter^{-/-} and Δ intron1^{-/-} NPCs, H3K4me3 was enriched on both parental chromosomes (Figure 4A), which agrees with the biallelic *Dlk1* expression in these cells (Figure 2C).

We assessed whether *Dlk1* activation in the WT NPCs correlated with enrichment of the serine-5-phosphorylated form of the CTD of RNA polymerase-II (PolIII-S5P), indicative of initiation of RNA transcription. At the KvDMR1, there was PolIII-S5P enrichment on the active paternal allele. At *Dlk1*, PolIII-S5P was precipitated at similar levels as at the housekeeping gene β -*Actin*, on the paternal allele predominantly (Figure 4B). Next, we performed ChIP on Δ promoter^{-/-} and Δ intron1^{-/-} NPCs. In these Meg3 RNA-deficient NPCs, the KvDMR1 showed unaltered PolIII-S5P enrichment on the paternal allele. At the *Dlk1* promoter, however, there was biallelic PolIII-S5P precipitation (Figure 4B).

To assess the *in vivo* relevance of the findings in NPCs, ChIP was performed on neonatal hypothalamus, a tissue in which

Figure 3. *Meg3* lncRNA Overlaps the Maternal *Dlk1* Gene in ESCs

- (A) Representative RNA FISH of MS2-tagged exon-10 of *Meg3* (green) in ESCs (line 2D1, see also Figure S3) with detection of main foci at transcription site (zoom-in, arrowheads), following ActD treatment. Right: representative RNA FISH for *Gata6*.
 (B) Main Meg3 RNA foci are present in most cells; many remain visible after 60 min of ActD treatment.
 (C) RNA FISH detection of MS2-tagged exon-10 of *Meg3* (red) in ESCs (line 2D1) and concomitant DNA FISH with the *Dlk1* fosmid (white) and a 20-kb fosmid comprising *Dio3* (green).
 (D) Pearson coefficients for *Meg3* RNA overlap with *Dlk1* and *Dio3* on the maternal chromosome (20 nuclei). ****p < 0.0001 (unpaired t test). Error bars indicate SD. See also Figure S3.



(legend on next page)

we had detected the highest levels of *Dlk1* expression (Figure 4C). Similarly as in WT NPCs, H3K4me3 and PolII-S5P were enriched on the paternal *Dlk1* promoter relative to the used input chromatin. Combined, the above studies indicate that the developmental activation of *Dlk1* involves RNA-PolII activation and H3K4me3, and *Meg3* expression prevents this process on the maternal chromosome.

We also explored H3K36me3 (Figure S4A), a modification linked to transcriptional elongation that can influence in different ways the establishment of H3K27me3 by the PRC2 complex (Cai et al., 2013; Schmitges et al., 2011). In WT and Δ promoter^{-/-} NPCs, as expected, at the control imprinted gene *Grb10* precipitation was maternal allele-specific (Figure S4A). At *Meg3*, the assessed exon-10 region showed considerable H3K36me3 precipitation in WT NPCs, on the maternal allele only. In the Δ promoter^{-/-} NPCs, which no longer express *Meg3*, there was an almost complete lack of H3K36me3. At *Dlk1*, at the 3'-most exon (*Dlk1*-3'), paternal enrichment was observed in WT NPCs, and biallelic enrichment in the Δ promoter^{-/-} NPCs. These findings indicate that H3K36me3 is linked to expression at both *Dlk1* and *Meg3*.

The PRC2 Complex Contributes to *Dlk1* Imprinting

PRC2-mediated H3K27me3 contributes to keeping developmental genes poised and, when CpG island-promoters are no longer expressed, many bind PRC2 complexes, possibly through the action of Polycomb-like proteins (Li et al., 2017; Riising et al., 2014).

Published ChIP-seq data on ESC and NPCs reveal a broad region of H3K27me3 enrichment around *Dlk1* (Figure S4B). In cross-linked chromatin of ESCs and NPCs, H3K27me3 precipitation at *Dlk1* was similarly high as at the repressed *Hoxa11* gene and *Grb10*, an imprinted gene marked by paternal H3K27me3 (Sanz et al., 2008). H3K27me3 at *Dlk1* seemed biallelic in both ESC and NPCs (Figures 5A and S4D). Concordantly, H3K27me3 precipitation levels at *Dlk1* were comparable in androgenetic and parthenogenetic ESCs (Figure S4C). In agreement with this finding, in ESCs, there was biallelic precipitation of Ezh2 at *Dlk1* (Figure S4D). In NPCs, Ezh2 precipitation, although lower than in ESCs, remained largely biallelic (Figure 5A).

Dlk1 encodes a cell surface protein, which allowed us to purify *Dlk1*-expressing cells by "magnetic activated cell sorting" (Figure S5A). Both in *Dlk1*-expressing (*Dlk1*⁺) and negatively sorted (*Dlk1*⁻) neural cells, H3K27me3 precipitation was apparent on both the parental chromosomes (Figure S5B). This indicates considerable H3K27me3 on both parental alleles at the gene, irrespective of levels of *Dlk1* expression.

Next, we explored H3K27 acetylation (H3K27ac), which is mutually exclusive with H3K27me3. In WT NPCs, in which *Dlk1* expression is paternal, H3K27ac was enriched on the paternal

Dlk1 promoter (Figures S4E and S5C). Allelic enrichment was not apparent at day 4 of differentiation, suggesting that acquisition of an active chromatin configuration occurs at the time of *Dlk1* activation. In the *Meg3* Δ promoter^{-/-} neural cells that express *Dlk1* from both the parental chromosomes, there was biallelic H3K27ac promoter enrichment (Figure S4E). Combined, these data suggest acquisition of H3K27ac at the activated paternal *Dlk1* promoter during ESC differentiation, while there is considerable maintenance of H3K27me3 at the region on both parental chromosomes.

To explore a possible involvement of PRC2 in *Dlk1* imprinting, first we used an inducible *Eed*^{-/-} ESC line (Ura et al., 2008). Two days after tetracycline-induced targeting, *Eed* was no longer detected, and at day 3, H3K27me3 was globally lost as well (Figure S6A). *Meg3* expression was unaltered in *Eed*^{-/-} cells and the lncRNA remained present as a large nuclear focus in the ESCs. *Mirg* and *Rian* expression was also unaltered (Figures S6B and S6C). ChIP showed absence of H3K27me3 at *Dlk1* in the *Eed*^{-/-} cells (Figure S6D). *Dlk1* expression was several-fold higher than in WT ESCs, suggesting a possible repressive role of PRC2 (Figure S6B).

Next, we performed gene targeting directly on *Ezh2* in the BJ ESCs. We did not ablate *Ezh2*, which affects PRC2 stability through loss of interaction with *Eed* and other PRC2 components (Han et al., 2007). Rather, we deleted the first start codon (in exon 2) to generate an isoform that initiates at the second start codon (in exon 3) and lacks the first 40 aa. Despite its intact SET domain (at the C terminus) and expression at physiological levels (Figure 5B), the smaller isoform (Δ Ezh2) gave an almost complete global loss of H3K27me3 (Figure 5B). As expected (Han et al., 2007), the expression of *Eed* was unaffected (Figure 5B). ChIP showed that the Δ Ezh2 protein was not recruited to the *Dlk1-Dio3* locus (Figure 5C), which agrees with an earlier study on the N terminus (Cha et al., 2005).

Expression of *Meg3*, *Rian*, and *Mirg* was unaffected by the *Ezh2* truncation and *Meg3* lncRNA foci were as in WT cells (Figures 5D and 5E). Concordantly, there was also unaltered DNA methylation at the *Meg3* promoter and the IG-DMR (Figure S6E).

Δ Ezh2 ESCs could be readily differentiated into neural cells, with a high proportion expressing Nestin and Tubb3 (Figures S6F and S6G). Differentiation had proceeded sufficiently to strongly induce *Dlk1* (Figure 5D). In the Δ Ezh2 NPCs obtained, there was biallelic *Dlk1* expression at day 12 and two further time points of differentiation (Figure 5F).

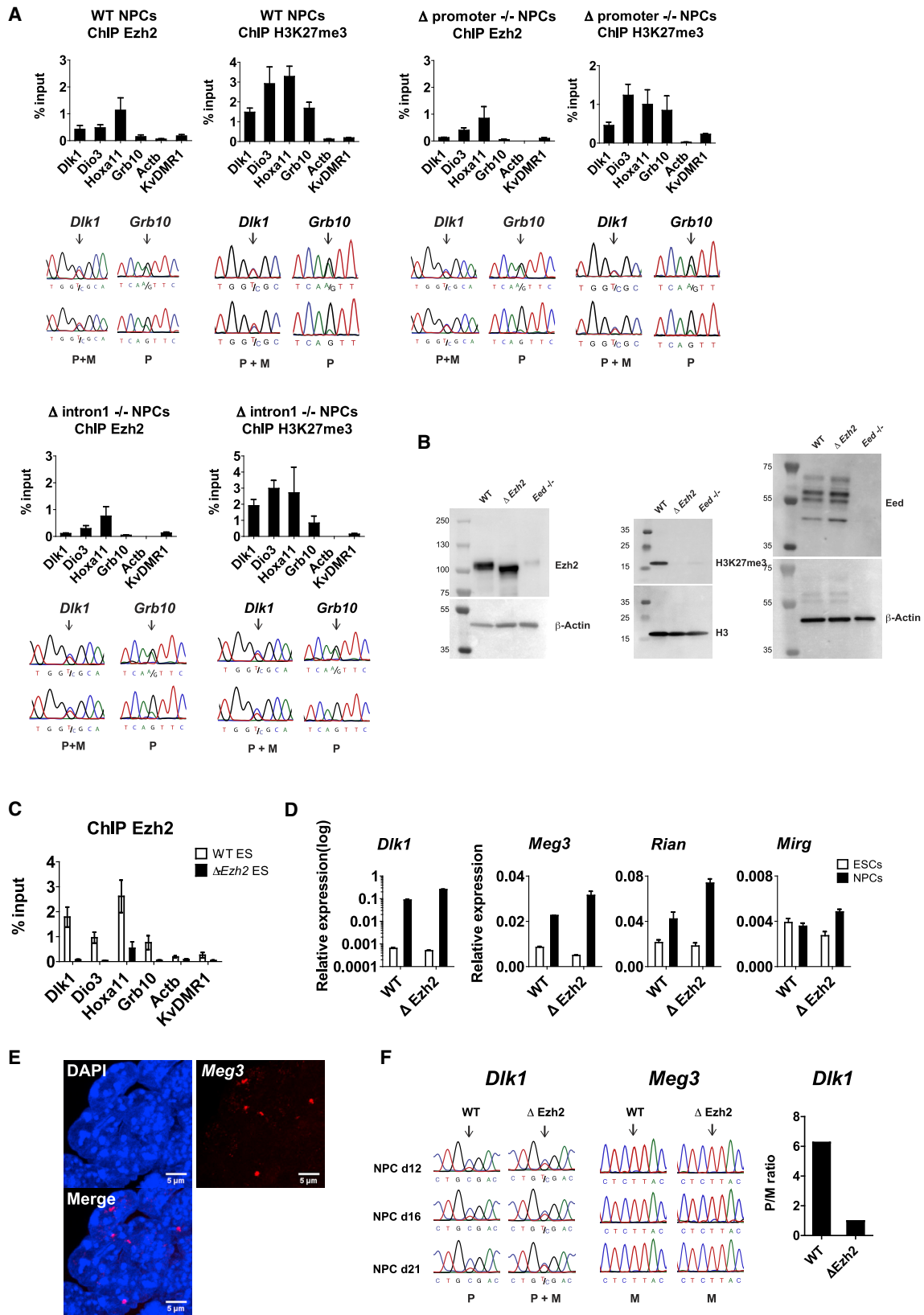
The above findings indicate that besides *Meg3* expression, KMT Ezh2 prevents *Dlk1* upregulation on the maternal chromosome during differentiation. Recruitment of Ezh2 to *Dlk1*, however, seemed independent of *Meg3* expression. In the *Meg3* Δ promoter^{-/-} and neural cells, there was unaltered biallelic Ezh2 recruitment to the *Dlk1* promoter region (Figure 5A).

Figure 4. *Meg3* Expression Prevents Active Chromatin Formation at *Dlk1*

(A and B) ChIP on WT, Δ promoter^{-/-}, and Δ intron1^{-/-} NPCs (d12) against H3K4me3 (A) and PolII-S5P (B). Levels of precipitation (% input chromatin) were determined by real-time PCR. Bottom: Sanger sequencing profiles show the allele-specificity of the precipitated chromatin at *Dlk1* and the control imprinted promoter KvDMR1. P, paternal chromosome; M, maternal chromosome.

(C) ChIP of H3K4me3 and PolII-S5P in neonatal hypothalamus (at P0). Quantification and allele-specificity assays were as for (A) and (B). Error bars indicate the SEM of qPCR triplicates.

See also Figures S4 and S5.



(legend on next page)

DISCUSSION

Our main finding is that *Dlk1* imprinted expression arises through upregulation of the paternal allele. The maternal allele remains poised and this is controlled *in cis* by expression of the *Meg3* polycistronic gene. Ezh2 contributes to the protection against developmental upregulation as well, although its recruitment to *Dlk1* is biallelic and does not depend on *Meg3* lncRNA. Despite the nuclear availability of transcription factors that control the developmental *Dlk1* activation, both *Meg3* expression and the PRC2 complex prevent such activation to occur on the maternal chromosome.

The *Meg3* RNA *cis* foci included different intronic sequences. Given that these main RNA foci were still detectable a considerable time after RNA-PolIII inhibition, this partial lack, or delay, of splicing may serve as a local-retention signal. A future challenge will be to assess whether the *Meg3* lncRNA itself plays a role in chromatin repression and which structure(s) might be involved. Our data, however, do not exclude a contribution of *Meg3* transcription (e.g., through transcription-linked H3K36me3 or other modifications on the maternal chromosome) that, in turn, could influence chromatin regulation elsewhere in the locus (Cai et al., 2013; Schmitges et al., 2011).

Paternal *Dlk1* activation is linked to RNA-PolIII phosphorylation and local acquisition of H3K4me3 and H3K27ac. These marks of active chromatin are not acquired on the maternal *Dlk1* promoter. Possibly, this is because *Meg3* lncRNA overlaps *Dlk1* *in cis* in embryonic cells and could thereby influence transcription factor binding or the efficacy of the PRC2 complex. Alternatively, the overlap of *Meg3* RNA and *Dlk1* results from the close proximity of the two loci but is functionally independent of PRC2. Our study provides no evidence for a role of PRC2 in *Meg3* expression, DNA methylation at the promoter or the lncRNA's localization, which contrasts with a recent report on constitutive *Ezh2*^{-/-} cells (Das et al., 2015).

Two earlier studies on mice used homologous recombination to generate deletions upstream and comprising *Meg3* (Takahashi et al., 2009; Zhou et al., 2010). Although of considerable interest, these led to opposite conclusions as to the role of *Meg3* in *Dlk1* imprinting. This may have been linked to the large sizes of the deleted regions or the non-removal of selection cassettes, which in one case still gave expression through the *Meg3* transcription unit, and in the other, transcription from the cassette toward the IG-DMR. Our CRISPR-Cas9 NHEJ approach did not yield such complications, and the *Dlk1* gene showed sense transcription only in both the WT and *Meg3* KO cells.

Many lncRNA genes enhance the expression of close-by protein-coding genes (Tan et al., 2017). This stimulatory effect occurs because the promoters of many lncRNA genes act as enhancers as well, and at some, because of the transcription itself (Engreitz et al., 2016). The action of *Meg3* is the exact opposite: its expression keeps close-by protein-coding gene(s) lowly expressed. It seems unlikely that the active *Meg3* promoter plays a role in this process.

Loss of *Meg3* expression correlated with an aberrant gain of DNA methylation at the maternal *Meg3* promoter. This protective role of *Meg3* expression agrees with the observation that in blastocysts this promoter acquires DNA methylation on the non-activated paternal allele (Kota et al., 2014; Sato et al., 2011). It also agrees with type 2 diabetes studies in which downregulation of *MEG3* correlated with acquisition of methylation at its promoter (Kameswaran et al., 2014).

Our findings are likely relevant to the imprinting disorder Kagami-Ogata syndrome (KOS14), which is often caused by paternal uniparental disomy of chromosome 14 (Ogata and Kagami, 2016). A minority of patients have maternal micro-deletions of *MEG3* promoter that do not affect the IG-DMR (Beygo et al., 2015). In one KOS14 family, a maternal micro-deletion left intact the IG-DMR and the *MEG3* promoter but affected the expression of the *MEG3* transcription unit (van der Werf et al., 2016). Although further studies are required, these human studies may agree with our finding that *Meg3* expression prevents activation of protein coding gene(s) on the maternal chromosome.

EXPERIMENTAL PROCEDURES

ESC Derivation and Differentiation

Hybrid ESCs were derived in serum-free (2i) medium with LIF, Mek inhibitor PD0325901 (1 μ M), and Gsk3 inhibitor CHIR99021 (3 μ M) and maintained in ESGRO 1i medium (LIF and Gsk3 inhibitor) (Millipore). Institutional Review Board approval for the usage of C57BL6/J and JF1 mice was obtained from the Reseaux Animalerie de Montpellier, Montpellier, France. ESC characterization and karyotyping were as described (Kota et al., 2014; Nagy et al., 2008). Lines BJ-WT3 and JB-WT2 are male; line JB-WT6 is female. Cells were differentiated into NPCs on Matrigel-coated dishes as described (Gaspard et al., 2009; Kota et al., 2014). Cyclopamine (1 μ M) was added during days 2–10 of differentiation. Retinoic acid (RA)-mediated ESC differentiation was performed by addition of all-trans RA (1 μ M) during days 2–10 of differentiation (Kim et al., 2009). For magnetic activated cell sorting, see the Supplemental Experimental Procedures.

CRISPR-Cas9 NHEJ-Mediated Deletions

Single guide RNAs (sgRNAs) (Table S3) were designed using CRISPR Design tool (<http://crispr.mit.edu/>), were synthesized with *BbsI* sticky ends and cloned

Figure 5. Ezh2 Contributes to *Dlk1* Imprinted Gene Expression

(A) Ezh2 and H3K27me3 ChIP on WT, Δ promoter^{-/-}, and Δ intron1^{-/-} NPCs (d12). Levels (% input chromatin) and the allele-specificity of precipitation were assayed as for Figure 4. The control imprinted gene, *Grb10*, has paternal allele-specific H3K27me3 and Ezh2 in neural cells (Sanz et al., 2008). In the quantifications, *Hoxa11* and *ActB* constitute positive and negative controls, respectively. Error bars indicate the SEM of qPCR triplicates.

(B) CRISPR-Cas9 deletion within exon-2 of *Ezh2* in BJ ESCs. Western blotting shows that the obtained 40 aa-truncated protein (Δ Ezh2) does not alter Eed expression, but gives loss of H3K27me3. As a control, *Eed*^{-/-} ESCs were included.

(C) ChIP on cross-linked chromatin of WT and Δ Ezh2 ESCs against the N-terminal part of Ezh2 (present both in the full-length and truncated Ezh2). Error bars indicate the SEM of qPCR triplicates.

(D) *Dlk1*, *Meg3*, *Rian*, and *Mirg* expression in WT and Δ Ezh2 NPCs at d12 of neural differentiation. Error bars indicate the SEM of qPCR triplicates.

(E) Sustained focal *Meg3* accumulation in Δ Ezh2 cells analyzed by smiFISH. Scale bars, 5 μ m.

(F) Allele-specificity of *Dlk1* and *Meg3* expression in WT and KO cells at days 12, 16, and 21 of neural differentiation in one representative differentiation experiment. Right: allelic quantitative PCR to assess *Dlk1* expression. See also Figure S6.

into pSpCas9(BB)-2A-GFP (Addgene, 48138). Constructs were transfected into BJ ESCs using Amaxa nucleofector (Lonza). 48 hr after transfection, GFP-positive cells were sorted by flow cytometry (FACS Aria, Becton Dickinson) and plated at low density (1,000 cells per 10-cm dish). After 7–8 days of culture, cell lines were established from single colonies.

RNA Expression and DNA Methylation Analysis

RNA expression and DNA methylation studies were as described before (Kota et al., 2014; Riso et al., 2016). Tables S1 and S2 describe the PCR primers used. Further details are in the Supplemental Experimental Procedures.

Chromatin Immunoprecipitation

Analysis of precipitated cross-linked chromatin is described in the Supplemental Experimental Procedures. Table S2 presents the PCR primers used.

Histone Extraction and Western Blotting

For total protein extraction, cells were lysed in RIPA buffer (Sigma) (30 min, on ice), centrifuged at 13,000 × g (15 min, 4°C); supernatants were quantified using the BCA protein assay (Thermo Scientific, 23227). Histone extraction and western blotting are presented in the Supplemental Experimental Procedures.

Fluorescence In Situ Hybridization and Immunofluorescence Studies

RNA-FISH was as described (Kota et al., 2014). Images were acquired on a laser scanning confocal microscope (LSM780, Zeiss) with 63×NA1.4 Plan-Apochromat objective (Zeiss). z stacks of 0.4-μm slices were analyzed using ImageJ software. RNA FISH against *Gata6* was with a BAC probe (RP23-129L1) (Miyanari and Torres-Padilla, 2012). For RNA-smiFISH, 24 oligonucleotides of 54–60 nt in length were designed to *Meg3* (Table S4) and synthesized with 28-nt “FLAP sequences” and were hybridized by secondary fluorescent probes as described (Tsanov et al., 2016). Simultaneous RNA and DNA FISH is explained in the Supplemental Experimental Procedures. Immunofluorescence staining of proteins was as described (Gaspard et al., 2009). Primary antibodies: anti-Nestin (Biolegend, 839801), anti-Tubb3 (Biolegend, 801201). Secondary antibodies: goat anti-mouse Alexa Fluor 488 (Life Technologies, A-11011), goat anti-rabbit Alexa Fluor 594 (Life Technologies, A-11012).

DATA AND SOFTWARE AVAILABILITY

The accession number for the RNA-seq data reported in this paper is GEO: GSE99903.

SUPPLEMENTAL INFORMATION

Supplemental Information includes Supplemental Experimental Procedures, six figures, and five tables and can be found with this article online at <https://doi.org/10.1016/j.celrep.2018.03.044>.

ACKNOWLEDGMENTS

We thank the “Montpellier Ressources Imagerie”; Marion Peters for assistance with smiFISH; Christina Pescia, Alice Marchand, and Patricia Cavellier for ESC derivation and culture; and Tristan Bouschet (IGF, Montpellier) for help with neural differentiation. Drs. Takashi Yokata (Kanazawa University, Ishikawa), Raphaël Margueron (Curie Institute, Paris), and Maria-Elena Torres-Padilla (Helmholtz Zentrum, Munich) kindly provided conditional *Eed*^{-/-} cells, anti-Ezh2 antiserum, and *Gata6* probe, respectively. R.F. acknowledges funding from the Agence Nationale de la Recherche (“Blanc” grant “Imprint-RNA”) and the Fondation Recherche Médicale (FRM) (DEQ20150331703), and his laboratory benefited from support by the Labex EpiGenMed, an “Investissement d’avenir” program (reference ANR-10-LABX-12-01). I.S. was salary-funded by the People Programme (Marie Curie Initial Training Network “INGENIUM”) of the EU 7th Framework Programme under the Research Executive Agency grant agreement 290123. S.L. acknowledges salary funding from Labex EpiGenMed and the University of Montpellier. A.R. acknowledges grant funding from Fondazione Telethon Italy (GGP11222).

AUTHOR CONTRIBUTIONS

Conceptualization, R.F., I.S., S.L., and E.B.; Methodology, S.L., E.B., and D.L.; Investigation, I.S., S.L., M.C., A.P., D.R., and F.R.; Formal Analysis, I.S., S.L., M.C., A.R., D.R., E.B., and R.F.; Writing – Original Draft, R.F.; Writing – Review & Editing, R.F., I.S., S.L., and A.R.; Funding Acquisition, R.F., E.B., and A.R.; Project Administration, R.F.; Supervision, R.F. and A.R.

DECLARATION OF INTERESTS

The authors declare no competing interests.

Received: June 14, 2017

Revised: December 1, 2017

Accepted: March 10, 2018

Published: April 10, 2018

REFERENCES

- Bensaude, O. (2011). Inhibiting eukaryotic transcription: which compound to choose? How to evaluate its activity? *Transcription* 2, 103–108.
- Beygo, J., Elbracht, M., de Groot, K., Begemann, M., Kanber, D., Platzer, K., Gillessen-Kaesbach, G., Vierzig, A., Green, A., Heller, R., et al. (2015). Novel deletions affecting the MEG3-DMR provide further evidence for a hierarchical regulation of imprinting in 14q32. *Eur. J. Hum. Genet.* 23, 180–188.
- Bouschet, T., Dubois, E., Reynès, C., Kota, S.K., Rialle, S., Maupetit-Méhouas, S., Pezet, M., Le Digarcher, A., Nidelet, S., Demolombe, V., et al. (2017). In vitro corticogenesis from embryonic stem cells recapitulates the in vivo epigenetic control of imprinted gene expression. *Cereb. Cortex* 27, 2418–2433.
- Cai, L., Rothbart, S.B., Lu, R., Xu, B., Chen, W.Y., Tripathy, A., Rockowitz, S., Zheng, D., Patel, D.J., Allis, C.D., et al. (2013). An H3K36 methylation-engaging Tudor motif of polycomb-like proteins mediates PRC2 complex targeting. *Mol. Cell* 49, 571–582.
- Cha, T.L., Zhou, B.P., Xia, W., Wu, Y., Yang, C.C., Chen, C.T., Ping, B., Otte, A.P., and Hung, M.C. (2005). Akt-mediated phosphorylation of EZH2 suppresses methylation of lysine 27 in histone H3. *Science* 310, 306–310.
- Charalambous, M., Da Rocha, S.T., Radford, E.J., Medina-Gomez, G., Curran, S., Pinnock, S.B., Ferrón, S.R., Vidal-Puig, A., and Ferguson-Smith, A.C. (2014). DLK1/PREF1 regulates nutrient metabolism and protects from steatosis. *Proc. Natl. Acad. Sci. USA* 111, 16088–16093.
- Cifuentes-Rojas, C., Hernandez, A.J., Sarma, K., and Lee, J.T. (2014). Regulatory interactions between RNA and polycomb repressive complex 2. *Mol. Cell* 55, 171–185.
- da Rocha, S.T., Edwards, C.A., Ito, M., Ogata, T., and Ferguson-Smith, A.C. (2008). Genomic imprinting at the mammalian Dlk1-Dio3 domain. *Trends Genet.* 24, 306–316.
- Das, P.P., Hendrix, D.A., Apostolou, E., Buchner, A.H., Canver, M.C., Beyaz, S., Ljuboja, D., Kuintzle, R., Kim, W., Karnik, R., et al. (2015). PRC2 is required to maintain expression of the maternal Gtl2-Rian-Mirg locus by preventing de novo DNA methylation in mouse embryonic stem cells. *Cell Rep.* 12, 1456–1470.
- Davidovich, C., Zheng, L., Goodrich, K.J., and Cech, T.R. (2013). Promiscuous RNA binding by Polycomb repressive complex 2. *Nat. Struct. Mol. Biol.* 20, 1250–1257.
- Engreitz, J.M., Haines, J.E., Perez, E.M., Munson, G., Chen, J., Kane, M., McDonel, P.E., Guttman, M., and Lander, E.S. (2016). Local regulation of gene expression by lncRNA promoters, transcription and splicing. *Nature* 539, 452–455.
- Falaleeva, M., Welden, J.R., Duncan, M.J., and Stamm, S. (2017). C/D-box snoRNAs form methylating and non-methylating ribonucleoprotein complexes: Old dogs show new tricks. *BioEssays* 39. <https://doi.org/10.1002/bies.201600264>.
- Gaspard, N., Bouschet, T., Herpoel, A., Naeije, G., van den Aemele, J., and Vanderhaeghen, P. (2009). Generation of cortical neurons from mouse embryonic stem cells. *Nat. Protoc.* 4, 1454–1463.

- Han, Z., Xing, X., Hu, M., Zhang, Y., Liu, P., and Chai, J. (2007). Structural basis of EZH2 recognition by EED. *Structure* 15, 1306–1315.
- Ito, M., Sferruzzi-Perri, A.N., Edwards, C.A., Adalsteinsson, B.T., Allen, S.E., Loo, T.H., Kitazawa, M., Kaneko-Ishino, T., Ishino, F., Stewart, C.L., and Ferguson-Smith, A.C. (2015). A trans-homologue interaction between reciprocally imprinted miR-127 and Rtl1 regulates placenta development. *Development* 142, 2425–2430.
- Kameswaran, V., Bramswig, N.C., McKenna, L.B., Penn, M., Schug, J., Hand, N.J., Chen, Y., Choi, I., Vourekas, A., Won, K.J., et al. (2014). Epigenetic regulation of the DLK1-MEG3 microRNA cluster in human type 2 diabetic islets. *Cell Metab.* 19, 135–145.
- Kaneko, S., Son, J., Shen, S.S., Reinberg, D., and Bonasio, R. (2013). PRC2 binds active promoters and contacts nascent RNAs in embryonic stem cells. *Nat. Struct. Mol. Biol.* 20, 1258–1264.
- Kaneko, S., Bonasio, R., Saldaña-Meyer, R., Yoshida, T., Son, J., Nishino, K., Umezawa, A., and Reinberg, D. (2014). Interactions between JARID2 and non-coding RNAs regulate PRC2 recruitment to chromatin. *Mol. Cell* 53, 290–300.
- Kim, M., Habiba, A., Doherty, J.M., Mills, J.C., Mercer, R.W., and Huettner, J.E. (2009). Regulation of mouse embryonic stem cell neural differentiation by retinoic acid. *Dev. Biol.* 328, 456–471.
- Kota, S.K., Llères, D., Bouchet, T., Hirasawa, R., Marchand, A., Begon-Pescia, C., Sanli, I., Arnaud, P., Journot, L., Girardot, M., and Feil, R. (2014). ICR noncoding RNA expression controls imprinting and DNA replication at the Dlk1-Dio3 domain. *Dev. Cell* 31, 19–33.
- Labielle, S., Marty, V., Bortolin-Cavaillé, M.L., Hoareau-Osman, M., Pradère, J.P., Valet, P., Martin, P.G., and Cavaillé, J. (2014). The miR-379/miR-410 cluster at the imprinted Dlk1-Dio3 domain controls neonatal metabolic adaptation. *EMBO J.* 33, 2216–2230.
- Li, H., Liefke, R., Jiang, J., Kurland, J.V., Tian, W., Deng, P., Zhang, W., He, Q., Patel, D.J., Bulyk, M.L., et al. (2017). Polycomb-like proteins link the PRC2 complex to CpG islands. *Nature* 549, 287–291.
- Lin, S.P., Youngson, N., Takada, S., Seitz, H., Reik, W., Paulsen, M., Cavaillé, J., and Ferguson-Smith, A.C. (2003). Asymmetric regulation of imprinting on the maternal and paternal chromosomes at the Dlk1-Gtl2 imprinted cluster on mouse chromosome 12. *Nat. Genet.* 35, 97–102.
- Luo, Z., Lin, C., Woodfin, A.R., Bartom, E.T., Gao, X., Smith, E.R., and Shilatifard, A. (2016). Regulation of the imprinted Dlk1-Dio3 locus by allele-specific enhancer activity. *Genes Dev.* 30, 92–101.
- Miyanari, Y., and Torres-Padilla, M.E. (2012). Control of ground-state pluripotency by allelic regulation of Nanog. *Nature* 483, 470–473.
- Moon, Y.S., Smas, C.M., Lee, K., Villena, J.A., Kim, K.H., Yun, E.J., and Sul, H.S. (2002). Mice lacking paternally expressed Pref-1/Dlk1 display growth retardation and accelerated adiposity. *Mol. Cell Biol.* 22, 5585–5592.
- Nagy, A., Gertsenstein, M., Vintersten, K., and Behringer, R. (2008). Karyotyping mouse cells. *Cold Spring Harb. Protoc.* 2008. <https://doi.org/10.1101/pdb.prot4706>.
- Ogata, T., and Kagami, M. (2016). Kagami-Ogata syndrome: a clinically recognizable upd(14)pat and related disorder affecting the chromosome 14q32.2 imprinted region. *J. Hum. Genet.* 61, 87–94.
- Riising, E.M., Comet, I., Leblanc, B., Wu, X., Johansen, J.V., and Helin, K. (2014). Gene silencing triggers polycomb repressive complex 2 recruitment to CpG islands genome wide. *Mol. Cell* 55, 347–360.
- Riso, V., Cammisa, M., Kukreja, H., Anvar, Z., Verde, G., Sparago, A., Acuzio, B., Lad, S., Lonardo, E., Sankar, A., et al. (2016). ZFP57 maintains the parent-of-origin-specific expression of the imprinted genes and differentially affects non-imprinted targets in mouse embryonic stem cells. *Nucleic Acids Res.* 44, 8165–8178.
- Sanz, L.A., Chamberlain, S., Sabourin, J.C., Henckel, A., Magnuson, T., Hugnot, J.P., Feil, R., and Arnaud, P. (2008). A mono-allelic bivalent chromatin domain controls tissue-specific imprinting at Grb10. *EMBO J.* 27, 2523–2532.
- Sato, S., Yoshida, W., Soejima, H., Nakabayashi, K., and Hata, K. (2011). Methylation dynamics of IG-DMR and Gtl2-DMR during murine embryonic and placental development. *Genomics* 98, 120–127.
- Schmitges, F.W., Prusty, A.B., Faty, M., Stützer, A., Lingaraju, G.M., Aiwezian, J., Sack, R., Hess, D., Li, L., Zhou, S., et al. (2011). Histone methylation by PRC2 is inhibited by active chromatin marks. *Mol. Cell* 42, 330–341.
- Takahashi, N., Okamoto, A., Kobayashi, R., Shirai, M., Obata, Y., Ogawa, H., Sotomaru, Y., and Kono, T. (2009). Deletion of Gtl2, imprinted non-coding RNA, with its differentially methylated region induces lethal parent-origin-dependent defects in mice. *Hum. Mol. Genet.* 18, 1879–1888.
- Tan, J.Y., Smith, A.A.T., Ferreira da Silva, M., Matthey-Doret, C., Rueedi, R., Sönmez, R., Ding, D., Kutalik, Z., Bergmann, S., and Marques, A.C. (2017). cis-acting complex-trait-associated lincRNA expression correlates with modulation of chromosomal architecture. *Cell Rep.* 18, 2280–2288.
- Tsanov, N., Samacoits, A., Chouaib, R., Traboulsi, A.M., Gostan, T., Weber, C., Zimmer, C., Zibara, K., Walter, T., Peter, M., et al. (2016). smiFISH and FISH-quant - a flexible single RNA detection approach with super-resolution capability. *Nucleic Acids Res.* 44, e165.
- Ura, H., Usuda, M., Kinoshita, K., Sun, C., Mori, K., Akagi, T., Matsuda, T., Koide, H., and Yokota, T. (2008). STAT3 and Oct-3/4 control histone modification through induction of Eed in embryonic stem cells. *J. Biol. Chem.* 283, 9713–9723.
- van der Werf, I.M., Buiting, K., Czeschik, C., Reyniers, E., Vandeweyer, G., Vanhaesebrouck, P., Lüdecke, H.J., Wiczorek, D., Horsthemke, B., Mortier, G., et al. (2016). Novel microdeletions on chromosome 14q32.2 suggest a potential role for non-coding RNAs in Kagami-Ogata syndrome. *Eur. J. Hum. Genet.* 24, 1724–1729.
- Wang, X., Goodrich, K.J., Gooding, A.R., Naeem, H., Archer, S., Paucek, R.D., Youmans, D.T., Cech, T.R., and Davidovich, C. (2017a). Targeting of polycomb repressive complex 2 to RNA by short repeats of consecutive guanines. *Mol. Cell* 65, 1056–1067.
- Wang, Y., Shen, Y., Dai, Q., Yang, Q., Zhang, Y., Wang, X., Xie, W., Luo, Z., and Lin, C. (2017b). A permissive chromatin state regulated by ZFP281-AFF3 in controlling the imprinted Meg3 polycistron. *Nucleic Acids Res.* 45, 1177–1185.
- Yevtdiyenko, A., Carr, M.S., Patel, N., and Schmidt, J.V. (2002). Analysis of candidate imprinted genes linked to Dlk1-Gtl2 using a congenic mouse line. *Mamm. Genome* 13, 633–638.
- Zhao, J., Ohsumi, T.K., Kung, J.T., Ogawa, Y., Grau, D.J., Sarma, K., Song, J.J., Kingston, R.E., Borowsky, M., and Lee, J.T. (2010). Genome-wide identification of polycomb-associated RNAs by RIP-seq. *Mol. Cell* 40, 939–953.
- Zhou, Y., Cheunschun, P., Nakayama, Y., Lawlor, M.W., Zhong, Y., Rice, K.A., Zhang, L., Zhang, X., Gordon, F.E., Lidov, H.G., et al. (2010). Activation of paternally expressed genes and perinatal death caused by deletion of the Gtl2 gene. *Development* 137, 2643–2652.